

White light generation by resonant nonradiative energy transfer from epitaxial InGaN/GaN quantum wells to colloidal CdSe/ZnS core/shell quantum dots

This article has been downloaded from IOPscience. Please scroll down to see the full text article.

2008 New J. Phys. 10 123001

(<http://iopscience.iop.org/1367-2630/10/12/123001>)

[The Table of Contents](#) and [more related content](#) is available

Download details:

IP Address: 139.179.137.123

The article was downloaded on 06/12/2008 at 07:17

Please note that [terms and conditions apply](#).

White light generation by resonant nonradiative energy transfer from epitaxial InGaN/GaN quantum wells to colloidal CdSe/ZnS core/shell quantum dots

Sedat Nizamoglu¹, Emre Sari¹, Jong-Hyeob Baek², In-Hwan Lee³ and Hilmi Volkan Demir^{1,4}

¹ Department of Electrical and Electronics Engineering and Department of Physics, Nanotechnology Research Center, and Institute of Materials Science and Nanotechnology, Bilkent University, Ankara, Turkey TR-06800

² Korea Photonics Technology Institute, Gwangju 500-460, Korea

³ School of Advanced Materials Engineering, Research Center of Industrial Technology, Chonbuk National University, Chonju 561-756, Korea

E-mail: volkan@bilkent.edu.tr

New Journal of Physics **10** (2008) 123001 (10pp)

Received 27 August 2008

Published 4 December 2008

Online at <http://www.njp.org/>

doi:10.1088/1367-2630/10/12/123001

Abstract. We propose and demonstrate white-light-generating nonradiative energy transfer (ET) from epitaxial quantum wells (QWs) to colloidal quantum dots (QDs) in their close proximity. This proof-of-concept hybrid color-converting system consists of chemically synthesized red-emitting CdSe/ZnS core/shell heteronanocrystals intimately integrated on epitaxially grown cyan-emitting InGaN/GaN QWs. The white light is generated by the collective luminescence of QWs and QDs, for which the dot emission is further increased by 63% with nonradiative ET, setting the operating point in the white region of CIE chromaticity diagram. Using cyan emission at 490 nm from the QWs and red emission at 650 nm from the nanocrystal (NC) luminophors, we obtain warm white light generation with a correlated color temperature of $T_c = 3135$ K and tristimulus coordinates of $(x, y) = (0.42, 0.39)$ in the white region. By analyzing the time-resolved radiative decay of these NC emitters in our hybrid system with a 16 ps time resolution, the luminescence kinetics reveals a fast ET with a rate of $(2 \text{ ns})^{-1}$ using a multiexponential fit with $\chi^2 = 1.0171$.

⁴ Author to whom any correspondence should be addressed.

Solid-state lighting (SSL) holds great promise worldwide for its environmental and financial benefits. For example, only in North America, SSL is predicted to reduce carbon emission by 258 million metric tons per year, saving an expected total of 80 billion euros annually [1]. Therefore, by considering its potential impact around the globe, SSL-based white light generation has attracted global attention in recent years. For SSL, the color conversion technique based on yellowish YAG phosphors has already been commercialized, which is currently the most commonly used approach [2]–[4]. In this method, the blue electroluminescence of InGaN/GaN light-emitting diodes (LEDs) optically pumps the yellowish phosphor, and consequently, the phosphor photoluminescence (PL) provides very broad band emission for color conversion, which in turn leads to white light perception by human eyes. Phosphors have the advantage of high quantum efficiency. However, the current technology suffers from comparatively low white light quality such as the cool white appearance with undesirably high correlated color temperature. Another problem is the low level of its optical absorption in blue, which requires the use of a rather thick color-converting film. Yet another issue is the undesired color changes observed in the optical properties of the generated white light with input power. Also, the broad emission spectrum of phosphors makes it relatively difficult to widely tune the emission spectrum of the generated white light as is required in different lighting applications.

On the other hand, as an alternative to phosphors, semiconductor quantum dot nanocrystals (QD-NCs) exhibit favorable optical properties for lighting and offer high-quality photometric performance as color converters. For example, NC luminophors feature conveniently widely tuneable emission using the quantum size effect, allowing for the precise control and modification of application-specific spectral content of illumination. But their quantum efficiency is not as high as that of phosphors in the solid-state film. To address this issue in SSL with NC emitters, we propose and demonstrate white-light-generating nonradiative energy transfer (ET) pumping of colloiddally synthesized semiconductor QDs from epitaxially grown semiconductor quantum wells (QWs) for efficient color conversion. To date nonradiative Förster-type ET of excitons and free carriers from a QW to NCs has previously been shown [5] and the temperature dependence of such an ET from QWs to QDs has further been investigated [6]. However, the use of Förster ET in white light generation has not been studied or demonstrated at all so far. In this respect, our work provides the first proof-of-concept demonstration of Förster resonant ET in generating white light to increase the overall pumping efficiency as an advancement in SSL.

As for the color-converting luminophors, we exploit the use of combinations of semiconductor NCs in SSL, because they exhibit strong optical absorption towards shorter wavelengths, high photostability, relatively narrow and symmetric PL with high photobleaching thresholds, and reasonably small spectral overlap between absorption and emission [7]–[9]. Furthermore, various deposition techniques including Langmuir–Blodgett, spin casting, drop casting and electrostatic layer-by-layer assembly can be conveniently employed to make optical quality thin films of these NCs. Because of their attractive properties, these quasi-zero-dimensional semiconductor materials have been investigated extensively both theoretically and experimentally [10]–[21]. For example, thanks mainly to the tuneable nature of their emission, they have been exploited in various hybrid white light applications to date. Combinations of CdSe/ZnS core/shell NCs hybridized on blue-emitting InGaN/GaN LEDs have been successfully demonstrated for warm white light generation with a high color rendering index [22, 23]. The dual hybridization of NCs and fluorescent polymers has also been realized to obtain good photometric properties [24]. A blue and green dual-color-emitting InGaN/GaN

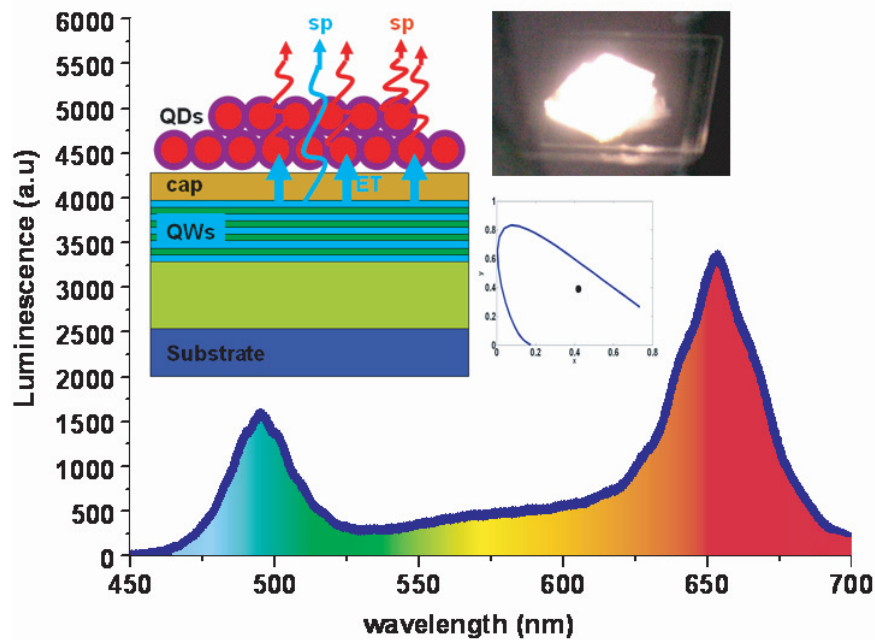


Figure 1. Luminescence spectrum of our hybrid color-converting system improved by using nonradiative ET pumping of red-emitting CdSe/ZnS core/shell NCs ($\lambda_{\text{PL}} = 650$ nm) by cyan-emitting InGaN/GaN QWs ($\lambda_{\text{PL}} = 490$ nm), along with the architecture of our hybrid system, its picture while generating white light, and its corresponding (x, y) tristimulus coordinates.

LED with red-emitting NCs, and a blue InGaN/GaN LED with yellow NCs and both red and green NCs have been reported [25, 26]. Also near-UV LEDs integrating a CdSeS NC mixture and a layer-by-layer assembly of CdSe/ZnS NCs in polymethyl methacrylate have been successfully realized [27]–[29]. Integration of dual-color-emitting QD–QW heteronanocrystals, made of CdSe/ZnS/CdSe in the core/shell/shell structure emitting red from the CdSe cores and green from the CdSe shells, on blue InGaN/GaN LEDs has also been demonstrated [30]. Furthermore, white-color-emitting CdS NCs from their surface states integrated on InGaN/GaN near-UV LEDs have been shown for tuneable high-quality white light generation [31, 32]. However, in all of these various white-light-generating examples, NC luminophors have only been optically pumped by the excitation LED platform; no energy transfer has been investigated or demonstrated for white light generation.

In this study, using nonradiative ET from epitaxial QWs to colloidal QDs, we present a proof-of-concept demonstration of enhanced white light generation. Our energy-transferring hybrid color conversion system consists of chemically synthesized red-emitting CdSe/ZnS core/shell nanocrystals integrated on epitaxially grown cyan-emitting InGaN/GaN QWs. The resulting white light is generated by the collective luminescence of the QWs and the NC emitters in which the NC emission is further increased by 63% with nonradiative ET, while setting the operating point in the white region of the CIE 1931 chromaticity diagram. Using the cyan emission from the QWs and red emission from the NC luminophors, we obtain warm white light generation with a correlated color temperature of $T_c = 3135$ K and tristimulus coordinates of $(x, y) = (0.42, 0.39)$ in the white region of the CIE chromaticity diagram as shown in figure 1.

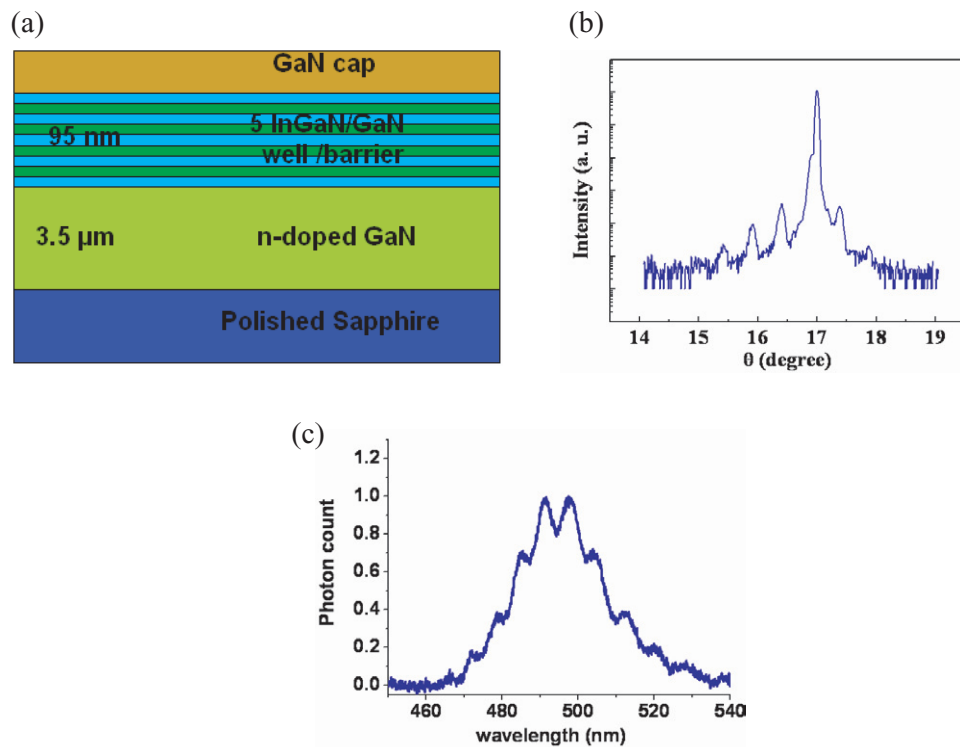


Figure 2. (a) Epitaxial structure of our cyan-emitting InGaN/GaN QW structure (not drawn to scale), (b) its XRD measurement and (c) its PL with its emission peak at 490 nm, excited at 325 nm.

By analyzing the time-resolved radiative decay of these NC emitters in our hybrid system, the luminescence kinetics shows a fast ET from QWs to QDs with a rate of $(2 \text{ ns})^{-1}$, which is faster than the typical radiative recombination rate of NCs (typically with a lifetime of tens of nanoseconds).

To achieve white light generation, we use InGaN/GaN semiconductor QWs and CdSe/ZnS core/shell QDs. For our InGaN/GaN wafer, we use our epitaxial design shown in figure 2(a) to emit at 490 nm. On top of the polished sapphire substrate we grow $3.5 \mu\text{m}$ thick n-doped GaN. Afterwards we continue with 5 InGaN/GaN well/barrier quantum structures and finally finish our structure with a few monolayers of undoped GaN capping layer with a thickness of a few nanometers. According to the x-ray diffraction (XRD) measurement in figure 2(b), the well and barrier thicknesses are about 95 nm with a well indium mole fraction of 83%. For steady-state measurements, we use a Jobin Yvon Triax 500 CCD PL system with an He/Cd laser at 325 nm; we show the resulting PL of our InGaN/GaN quantum structure in figure 2(c). Its peak emission is at 490 nm; the observed wavy PL stems from the phase separation in the quantum wells and barriers.

For QDs, we use CdSe/ZnS heteronanocrystals that emit at 650 nm. The diameters of these QDs are about 5.8 nm with a size dispersion of $< 5\%$; their transmission electron microscopy (TEM) image is presented in figure 3(a). As we observe in the TEM image, the shapes of these QDs are not perfectly spherical. Using He/Cd laser at 325 nm, the PL of these NCs is obtained with its emission peak around 650 nm as shown in figure 3(b). Since the optical absorption of

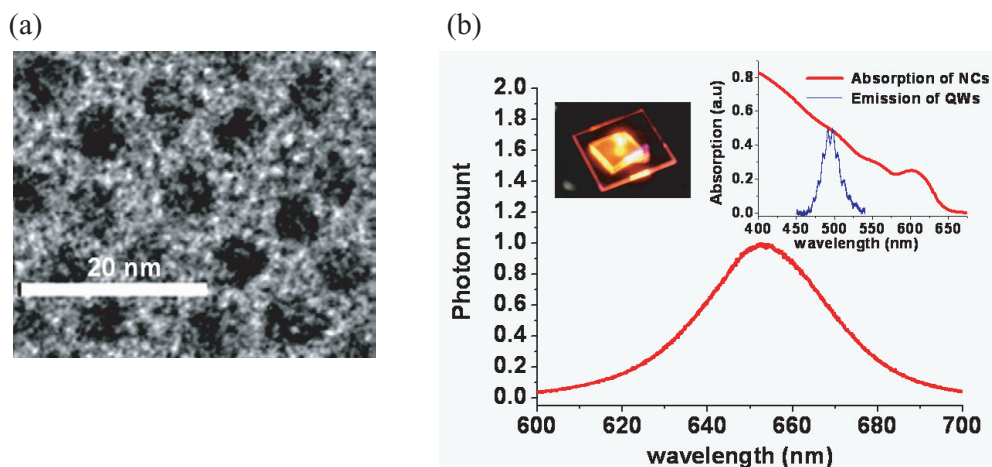


Figure 3. (a) TEM image and (b) PL of our NC luminophors excited at 325 nm, along with the optical absorption of these NCs and the emission spectrum of the QWs; inset: a photograph of the NCs while emitting at 650 nm.

the NCs increases towards shorter wavelengths, as shown in the inset of figure 3(b), the overlap of the NC absorption and the QW emission makes the dipole–dipole interaction between these NCs and QWs possible. For our hybrid structure and its negative control group, we use the same batch of NC dispersion in toluene with a concentration of $15.85 \text{ nmol ml}^{-1}$ and drop-cast the same amount of NC dispersion ($3 \mu\text{l}$) both on InGaN/GaN quantum well/barrier substrate and on quartz substrate, respectively (both with an area of 1 cm^2) by evaporating the excess solvent on the samples in a controlled environment. Consequently, on both samples, we obtain the same average film thickness of 270 nm, as measured by using an atomic force microscope (AFM), which is also consistent with the predicted film thickness of $<300 \text{ nm}$ by considering TOPO ligands of $<2 \text{ nm}$.

In figure 4, the steady-state PL spectra of our hybrid color-converting system that contains NCs integrated on QWs and that of its negative control group that includes only the NCs are shown. We observe that the emission of the NCs in the hybrid system is increased by 63% with respect to the case of only NCs as a result of the ET from the QWs to the NCs. Furthermore, in the hybrid system the emission of the NCs is disturbed, resulting in an asymmetric spectral emission profile, which is another evidence of the ET from the QWs to the QDs. It is a known fact that there exists homogeneous ET among the NCs due to their finite size distribution ($<5\%$), but this kind of ET would not yield such a wavy looking, asymmetric PL spectrum. Here, cyan-emitting QWs and red-emitting NCs are carefully selected to provide the operating point in the white region. For white light generation using dual-color emission, the line that connects primary emission wavelengths needs to intersect the white region, as a first requirement. As shown in the inset of figure 4, the connecting line of cyan and red emission passes through the white region, making it possible to obtain our operating point in the white region. As a second requirement, the ratio of the contributions from these two primary wavelengths also needs to be properly designed to balance out their contributions and fall in the white region of the chromaticity diagram. In this implementation, we achieve tristimulus coordinates of $(x, y) = (0.42, 0.39)$ with a correlated color temperature of $T_c = 3135 \text{ K}$ in the white region. Here, the ET provides a color balancing mechanism that maintains the operating point in the

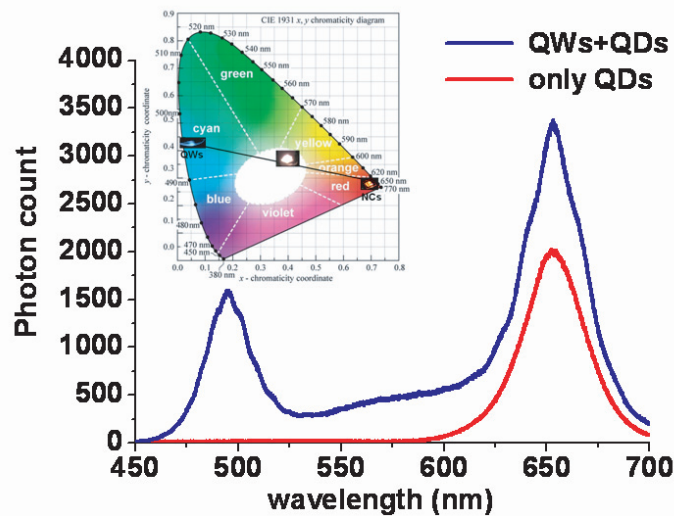


Figure 4. Steady-state emission spectrum of our hybrid system (QWs+QDs) improved by using nonradiative ET pumping of red-emitting CdSe/ZnS core/shell QDs ($\lambda_{PL} = 650$ nm) by cyan-emitting InGaN/GaN QWs ($\lambda_{PL} = 490$ nm) with respect to the case of only QDs, along with the CIE 1931 chromaticity diagram (inset) showing the resulting (x, y) tristimulus operating point and the connecting line of the primary emission wavelengths.

white region, while also shifting the tristimulus coordinates toward a warmer color temperature. Furthermore, it is also worth mentioning that, although we did not observe any stability problem during our experiments, we did not perform any stability measurement. However, it is well known that packaged InGaN/GaN QWs can operate for hundreds of thousands of hours. Core/shell heteronanocrystals also exhibit good photostability; they are compared with commonly used color converters such as rhodamine, fluorescein and Alexa-Fluor. This makes such NCs attractive among various color converters [30]. Thus, it is expected that this hybrid system should have reasonably high stability.

In this color-converting hybrid structure, the ET is a result of solely the dipole–dipole interaction between the QWs and the QDs, rather than the delocalized behavior of excitons or free carriers, since ZnS barriers of our QDs prevent tunneling and provide full electronic isolation [33]. In the previous studies by our group and others [22]–[32], white light generation has been achieved on the excitation platforms, where first the radiative recombination process occurs in QWs and, subsequently, their emitted photons excite luminophors that further luminescence via radiative recombination. In other words, there exist two cascaded radiative recombination processes required to emit photons from luminophors and generate white light. On the other hand, unlike these previous works, the advantage of our energy-transferring hybrid structure is that additional recombination takes place directly in the NCs (i.e. after the QWs transfer their excitation energy to the luminophor QDs for the recombination process to directly take place in the dots) for white light generation. Therefore, using nonradiative ET in white light generation facilitates an additional pathway for a direct, more efficient, single-stage process, as opposed to merely optical pumping that requires two stages of radiative recombination.

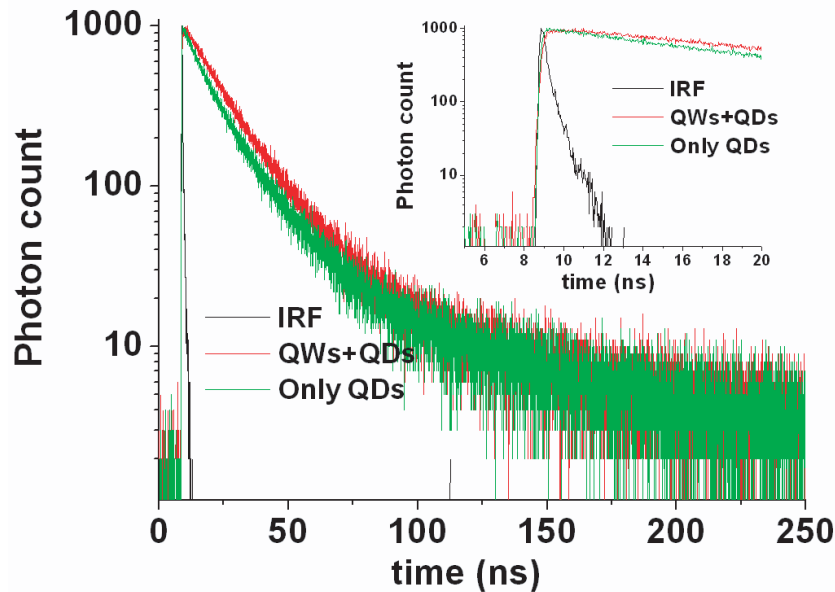


Figure 5. Time resolved spectroscopy measurement of our hybrid system that consists of both QWs and QDs (QWs + QDs), compared with that of the negative control group that contains only QDs (only QDs), along with the IRF of the laser diode emitting at 375 nm, using a TCSPC system of PicoHarp 300 with a time resolution of 16 ps.

For the time resolved spectroscopy measurements, we use a FluoTime 200 spectrometer from PicoQuant with a time-correlated single photon counting (TCSPC) system of PicoHarp 300. For pumping, we use a laser head emitting at 375 nm and a photon multiplier tube (PMT) as the detector. For the data analysis we use the software of FluoFit to retrieve the fitting decay parameters. In these measurements, our time resolution is 16 ps, which is sufficiently short to resolve the desired luminescence kinetics. Here, for a conclusive characterization of the energy transfer, we investigate our hybrid system particularly for emission at 650 nm to determine the energy transfer to the QDs and the resulting energy feeding in their luminescence, rather than studying the quenching of the QWs. This is because the quenching can occur also because of environmental impurities and conditions. However, the energy feeding in the luminescence of QDs can conclusively occur only as a result of the energy transfer to them. Figure 5 shows the time resolved spectroscopy of our hybrid system and only the NC solids as the control group. In the hybrid structure, the transient luminescence shows a smoother turnaround from the rising edge to the decaying tail (from 8 to 10 ns) because of the energy-transfer feeding component of the luminescence, as also zoomed in the inset of figure 5.

For the decay fits, we use a multiexponential least square error model, also being convoluted with the laser diode response (instrument response function (IRF)), as shown in equation (1). For only NCs, we use a double exponential fit, resulting in a good χ^2 near unity ($\chi^2 = 0.9369$), confirming that this is numerically a good fit. Here, for only NCs, the extracted lifetimes are 12.87 and 49.99 ns, as also presented in table 1. This 12.87 ns decay component corresponds to the typical lifetime of NCs, which is typically observed to be of the order of tens

Table 1. The multiexponential fitting parameters for the negative control group consisting of only QDs (only QDs) and our hybrid system consisting of both QWs and QDs (QWs+QDs).

	A_1	τ_1 (ns)	A_2	τ_2 (ns)	A_3	τ_3 (ns)
Only QDs	88.30	49.99	1120.90	12.87	–	–
QWs+QDs	102.35	49.99	1174.70	12.87	–200.00	2.00

of nanoseconds [34]–[36]. There is also another decay lifetime of 49.990 ns, which is rather long. However, the amplitude of this slow decay component is relatively weak with its amplitude of 88.30 units, compared with that of the typical 12.87 ns radiative decay (with 1120.90 units). This slow decay component is attributed to the emission through trap states. On the other hand, when we analyze our white light generating hybrid system of QWs+QDs together, we observe again two of these exponential decays with the same lifetimes of 12.87 and 49.99 ns as in the case of only NCs. However, we also observe an additional third exponential with a lifetime of 2.00 ns, having a negative amplitude this time (which implies an energy increase), as summarized in table 1. Such a negative amplitude is a unique characteristic of the resonant energy transfer. The fitting parameters used in the analysis of the hybrid system also yields a good χ^2 around unity ($\chi^2 = 1.0171$), again confirming an excellent fit. This short lifetime of the increasing emission component of 2.00 ns in the white-light-generating hybrid system implies that the energy transfer is faster than the recombination lifetime of these NCs with 12.87 ns. Consequently, the overall associated photon lifetime of the hybrid system increases; for example, the intensity weighted average time constant of the hybrid system, at 650 nm, is increased to 22.67 ns, when compared with the case of only NCs with 21.56 ns, and the white light generation is enhanced with respect to the case of only NCs.

$$I(t) = \int_{-\infty}^t \text{IRF}(t') \sum_{i=1}^n A_i \exp\left(-\frac{t-t'}{\tau_i}\right) dt'. \quad (1)$$

In conclusion, we have presented in this paper proof-of-concept white-light-generating nonradiative ET pumping of colloidal QD luminophors by epitaxial QWs. Using the ET from the wells to the dots, we achieved warm white light generation with a correlated color temperature of $T_c = 3135$ K and tristimulus coordinates of $(x, y) = (0.42, 0.39)$ in the white region by obtaining a 63% increase in the NC emission as a result of the ET. We strongly believe that such a white light generation enhanced with nonradiative energy transfer from QWs to NC luminophors holds great promise for future lighting applications.

Acknowledgments

This work was supported by EU-PHOREMOST NoE 511616, EU-MC-IRG MOON 021391 and TUBITAK under project numbers 107E297, 106E020, 104E114, 107E088, 105E065 and 105E066. Also, HVD acknowledges additional support from European Science Foundation European Young Investigator Award (ESF-EURYI) and Turkish Academy of Sciences Distinguished Young Scientist Award (TUBA-GEBIP) programs. We also acknowledge the

use of the facilities in the Bilkent University Nanotechnology Research Center (founder: Professor E Ozbay) and Advanced Research Laboratories and Institute of Materials Science and Nanotechnology (founder: Professor S Ciraci).

References

- [1] The Promise of Solid State Lighting for General Illumination Light Emitting Diodes (LEDs) and Organic Light Emitting Diodes (OLEDs) (Washington, DC: Optoelectronics Industry Development Association) http://www.netl.doe.gov/ssl/PDFs/oida_led-oled_rpt.pdf
- [2] Schubert E F 2006 *Light-Emitting Diodes* (Cambridge: Cambridge University Press)
- [3] Yamada M, Narukawa Y, Tamaki H, Murazaki Y and Mukai T 2005 *IEICE Trans. Electron.* **E88-C** 1860
- [4] Chen H, Yeh D, Lu C, Huang C, Shiao W, Huang J, Yang C C, Liu I and Su W 2006 *IEEE Photonics Technol. Lett.* **18** 1430
- [5] Achermann M, Petruska M A, Kos S, Smith D L, Koleske D D and Klimov V I 2004 *Nature* **429** 642
- [6] Rohrmoser S, Baldauf J, Harley R T, Lagoudakis P G, Sapra S, Eychmüller A and Watson I M 2007 *Appl. Phys. Lett.* **91** 092126
- [7] Gaponenko S 1998 *Optical Properties of Semiconductor Nanocrystals* (Cambridge: Cambridge University Press)
- [8] Clapp A R, Medintz I L and Mattoussi H 2006 *ChemPhysChem* **7** 47–57
- [9] Klimov V I, Mikhailovsky A, Xu S, Malko A, Hollingsworth J, Leatherdale C and Bawendi M 2000 *Science* **290** 314–7
- [10] Achermann M, Petruska M A, Crooker S A and Klimov V I 2003 *J. Phys. Chem. B* **107** 13782
- [11] Achermann M, Petruska M A, Koleske D D, Crawford M H and Klimov V I 2006 *Nano Lett.* **6** 1396
- [12] Franzl T, Shavel A, Rogach A L, Gaponik N, Klar T A, Eychmüller A and Feldmann J 2005 *Small* **1** 392
- [13] Somers R C, Bawendi M G and Nocera D G 2007 *Chem. Soc. Rev.* **36** 579–91
- [14] Mutlugun E, Soganci I M and Demir H V 2007 *Opt. Express* **15** 1128–34
- [15] Soganci I M, Nizamoglu S, Mutlugun E, Akin O and Demir H V 2007 *Opt. Express* **15** 14289–98
- [16] Sahin M and Tomak M 2005 *Phys. Rev. B* **72** 129904
- [17] Gaponenko S V, Woggon U, Saleh M, Langbein W, Uhrig A and Klingshirm C 1993 *J. Opt. Soc. Am. B* **10** 1947
- [18] Gaponik N P, Talapin D V and Rogach A L 1999 *Phys. Chem. Chem. Phys.* **1** 1787
- [19] Sahin M 2008 *Phys. Rev. B* **77** 119901
- [20] Artemyev M V, Bibik A I, Gurinovich L I, Gaponenko S V and Woggon U 1999 *Phys. Rev. B* **60** 1504
- [21] Gaponenko S V, Bogomolov V N, Petrov E P, Kapitonov A M, Eychmüller A, Rogach A L, Kalosha I I and Woggon U 2000 *J. Lumin.* **87–89** 152–6
- [22] Nizamoglu S, Ozel T, Sari E and Demir H V 2007 *Nanotechnology* **18** 065709
- [23] Nizamoglu S, Zengin G and Demir H V 2008 *Appl. Phys. Lett.* **92** 031102
- [24] Demir H V, Nizamoglu S, Ozel T, Mutlugun E, Huyal I O, Sari E, Holder E and Tian N 2007 *New J. Phys.* **9** 362
- [25] Chen H, Yeh D, Lu C, Huang C, Shiao W, Huang J, Yang C C, Liu I and Su W 2006 *IEEE Photonics Technol. Lett.* **18** 1430
- [26] Chen H, Hsu C and Hong H 2006 *IEEE Photonics Technol. Lett.* **18** 193
- [27] Ali M, Chattopadhyay S, Nag A, Kumar A, Sapra S, Chakraborty S and Sarma D D 2007 *Nanotechnology* **18** 075401
- [28] Nizamoglu S and Demir H V 2007 *Nanotechnology* **18** 405702
- [29] Nizamoglu S and Demir H V 2007 *J. Opt. A: Pure Appl. Opt.* **9** S419–24
- [30] Nizamoglu S, Mutlugun E, Özel T, Demir H V, Sapra S, Gaponik N and Eychmüller A 2008 *Appl. Phys. Lett.* **92** 113110

- [31] Demir H V, Nizamoglu S, Mutlugun E, Özel T, Sapra S, Gaponik N and Eychmüller A 2008 *Nanotechnology* **19** 335203
- [32] Nizamoglu S, Mutlugun E, Akyuz O, Kosku Perkgoz N, Demir H V, Liebscher L, Sapra S, Gaponik N and Eychmüller A 2008 *New J. Phys.* **10** 023026
- [33] Nizamoglu S and Demir H V 2008 *Opt. Express* **16** 3515–26
- [34] Kagan C R, Murray C B, Nirmal M and Bawendi M G 1996 *Phys. Rev. Lett.* **76** 1517–20
- [35] Kagan C R, Murray C B and Bawendi M G 1996 *Phys. Rev. B* **54** 8633–43
- [36] Crooker S A, Hollingsworth J A, Tretiak S and Klimov V I 2002 *Phys. Rev. Lett.* **89** 186802